Primary productivity of phytoplankton and its influencing factors in cold and arid regions : A case study of Wuliangsuhai Lake, China

Yu, Haifeng

2022-11

Yu , H , Shi , X , Zhao , S , Sun , B , Liu , Y , Arvola , L , Li , G , Wang , Y , Pan , X , Wu , R & Tian , Z 2022 , ' Primary productivity of phytoplankton and its influencing factors in cold and arid regions : A case study of Wuliangsuhai Lake, China ' , Ecological Indicators , vol. 144 , 109545 . https://doi.org/10.1016/j.ecolind.2022.109545

http://hdl.handle.net/10138/350644
https://doi.org/10.1016/j.ecolind.2022.109545

Ecological Indicators 144 (2022) 109545

Contents lists available at ScienceDirect

Ecological Indicators

journal homepage: www.elsevier.com/locate/ecolind

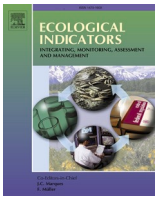

Original Articles

Primary productivity of phytoplankton and its influencing factors in cold and arid regions: A case study of Wuliangsuhai Lake, China

Haifeng Yu [a], Xiaohong Shi [a,b,c,*], Shengnan Zhao [a,b], Biao Sun [a,b], Yu Liu [a], Lauri Arvola [d], Guohua Li [a], Yanjun Wang [a], Xueru Pan [a], Rong Wu [a], Zhiqiang Tian [a]

[a] Water Conservancy and Civil Engineering College of Inner Mongolia Agricultural University, Hohhot 010018, China
[b] Inner Mongolia Water Resource Protection and Utilization Key Laboratory, Hohhot 010018, China
[c] State Gauge and Research Station of Wetland Ecosystem, Wuliangsuhaihai Lake, Inner Mongolia, Bayan Nur 014404, China
[d] Lammi Biological Station, Ecosystems and Environment Research Program, Faculty of Biological and Environmental Sciences, University of Helsinki, Lammi 00560, Finland

ARTICLE INFO

Keywords:
Wuliangsuhai Lake
Vertically generalized production model
Primary productivity
Environmental factors

ABSTRACT

This study measured the primary productivity (PP_{eu}) of phytoplankton in Wuliangsuhai Lake from April 2014 to January 2019 based on the monitoring and on-site exploration of 20 sampling points in the entire lake using a vertically generalized production model (VGPM). The relationship between the spatiotemporal variation in PP_{eu} and environmental factors was also analyzed. Our findings indicated that the temporal heterogeneity of PP_{eu} was strong, and the average annual PP_{eu} of the four seasons was significantly different ($P < 0.05$, $F = 54.74$), exhibiting the following descending order: summer (1279.89 ± 111.04 mg C•m^{-2}•d^{-1}) > spring (782.42 ± 59.34 mg C•m^{-2}•d^{-1}) > autumn (465.03 ± 49.30 mg C•m^{-2}•d^{-1}) > winter (96.34 ± 10.36 mg C•m^{-2}•d^{-1}). Even in winter with harsh environmental conditions, PP_{eu} under the ice sheet can reach 8 % of that in summer. The spatial heterogeneity was weak, and only the average annual PP_{eu} in spring exhibited a significant spatial difference ($P < 0.05$, $F = 5.18$): north > central > south. However, there were no significant differences in other seasons. Redundancy analysis (RDA) and multiple linear regression (MLR) results showed that in addition to directly participating in the calculation of the environmental factors of PP_{eu}, PP_{eu} in spring was mainly affected by total nitrogen (TN), total phosphorus (TP), and dissolved oxygen (DO). PP_{eu} in summer was mainly affected by dissolved inorganic phosphorus (DIP), dissolved oxygen (DO), salinity (S), electrical conductivity (EC), and water temperature (WT). PP_{eu} in autumn was mainly affected by pH, electrical conductivity (EC), suspended solids (SS), and water temperature (WT). PP_{eu} in winter was mainly affected by water temperature (WT) and ice thickness (IT). The mechanisms through which environmental factors affect primary productivity are complex and dynamic. Therefore, long-term monitoring and research of PP_{eu} in Wuliangsuhai Lake are necessary to explore the adaptation strategies of phytoplankton in ice and ice-free periods and understand the operation of natural life support systems under the alternation of ice generation and extinction. In turn, this would facilitate the development of strategies to maintain phytoplankton biodiversity and prevent algal blooms.

1. Introduction

The net primary productivity of phytoplankton can reach 50 % of the total biosphere (Behrenfeld et al., 2006), which is the basis for the energy flow of the food chain in aquatic ecosystems. Current research on primary productivity of phytoplankton has focused on tropical, subtropical and temperate lakes. Previous studies have shown that the primary productivity of phytoplankton is affected by inorganic turbidity, the synergistic effect of heavy metals and nutrients, and the monitoring location and depth (Schagerl and Oduor, 2003; Jia et al., 2020; Westernhagen et al., 2010). However, there are relatively few studies on the primary productivity of phytoplankton in cold and arid regions.

Current research on the primary productivity of the ice period has primarily focused on the polar regions and marine environments. Most of the polar and sea ice is covered by snow all year round. At this time, the temperature drives the deformation of the snow, resulting in changes in the optical properties of snow, and allowing sufficient light to

* Corresponding author.
E-mail address: imaushixiaohong@163.com (X. Shi).

https://doi.org/10.1016/j.ecolind.2022.109545
Received 18 July 2022; Received in revised form 3 October 2022; Accepted 5 October 2022
Available online 8 October 2022

penetrate the snow to drive the growth of algae under the ice. For example, the growth of algae under the sea ice in Greenland has extremely low light requirements (Hancke et al., 2018). Hoare Lake and Vanda Lake in the Antarctic are covered by ice all year round. The light transmittance of the ice sheet of these lakes is 18 % and 2 %, respectively, and the phytoplankton in the subglacial water is dominated by cyanobacteria (Hawes and Schwarz, 2001). It can be seen that the limitation of light on the growth and reproduction of phytoplankton may be limited in ice period.

With 50 million lakes freezing worldwide every year, lake ice cover is critical to protect the global freshwater supply (Sharma et al., 2021). Due to the presence of ice sheets, subglacial primary productivity can reorganize energy flows to provide energy to consumers in energy-scarce ecosystems during the ice period, thus affecting the annual primary productivity of aquatic ecosystems (Bondarenko et al., 2006). Currently, some researches on ice period have focused on ice luminous flux, ice extinction coefficient, and ice surface albedo (Grenfell and Perovich, 1984; Brown et al., 1995; Perovich, 2003). Other studies focus on the variations of physicochemical parameters (Guo et al., 2011; Terzhevik et al., 2009), Chlorophyll-a (Hampton et al., 2017), Ice-water nutrient migration (Canfield et al., 1983), and phytoplankton communities (Popovskaya, 2000). Few studies have been seen on phytoplankton primary productivity that include ice-free and ice periods.

Currently, the main methods for estimating phytoplankton primary productivity include the black and white bottle method (Pratt and Berkson, 1959), the isotope method (Cox et al., 2015), the empirical model method (Lan et al., 2020), and the remote sensing inversion method (Delu et al., 2005; Huan et al., 2021). The advantage of empirical model estimation is that it can better reflect the spatial and temporal distribution characteristics of phytoplankton primary productivity. Falkowski and Behrenfeld constructed the vertical generalized production model (VGPM) (Behrenfeld and Falkowski, 1997), and this model has since become the most widely adopted method for the estimation of primary productivity (Lakshmi et al., 2014; Everett and Doblin, 2015).

Inland lakes are among the water bodies that are most seriously affected by human activities, and are characterized by high nutrient concentration, frequent algal blooms, and high levels of primary productivity. Inland lakes also play a crucial role in the global energy circulation dynamics. From the perspective of lake ecology, studying the adaptation strategies of phytoplankton in the glacial period with low light, high nutrition, and ice cover and the ice-free period with high light, low nutrition, and no ice cover would provide crucial insights into the responses of natural phytoplankton communities to the alternating action of ice generation and elimination. We assume that the phytoplankton under the Wuliangsuhai Lake ice sheet can still grow and reproduce during the ice period, and the primary productivity of phytoplankton is not at the low level we expected, and there may be a high level of potential, and try to verify this conclusion. Therefore, from April 2014 to January 2019, monitoring and on-site investigation were carried out in Wuliangsuhai Lake, and the VGPM was used to calculate the primary productivity of phytoplankton across four seasons. Environmental factors affecting the primary productivity of phytoplankton during the ice period and ice-free period were analyzed by redundancy analysis (RDA) and multiple linear regression (MLR).

2. Materials and methods

2.1. Study area

Wuliangsuhai Lake (40°36′–41°03′N, 108°43′–108°57′E) is located in Bayan Nur, Inner Mongolia. It is a drainage lake of the Hetao Irrigation District, covering an area of approximately 325.31 km^2, with a water storage capacity of approximately 2.5–3 × 10^8 m^3 and an average water depth of 2.16 m (Song et al., 2019). The lake is located in the arid and semi-arid monsoon climate zone, with hot summers and extremely cold winters. The average annual rainfall and evaporation are approximately 224 mm and 1502 mm, respectively. The ice period lasts approximately 5 months, and the ice thickness can reach 0.3–0.6 m, freezing in early November and melting in early April of the following year.

2.2. Sample collection and data sources

Based on the mean temperature of the research area, the four seasons were divided. The sampling frequency is once a quarter, and the sampling times for spring, summer, autumn and winter are April, July, October, and January, respectively. A total of 20 sampling points were set up in the entire lake, as shown in Fig. 1 (the northern part of the lake is covered with reeds, and therefore no sampling points were set up). After positioning by GPS, water samples were collected at 0.5 m below the water surface (or the ice-water interface) of the sampling point with a water sampler, and use double parallel samples for sample collection, stored in two 1 L polyethylene bottles (after pickling, the sample was disinfected with 70 % alcohol), and transported back to the laboratory in a 4 °C incubator. A total of 800 water samples were collected over a 20-month period.

The index detection methods used in this study are shown in Table 1. If the relative deviation of the test results of the two groups was <10 %, the average value was taken as the monitoring value, otherwise the test was re-measured. Water Temperature (WT), Salinity (S), pH, Electrical Conductivity (EC), Total Dissolved Solids (TDS), Dissolved Oxygen (DO), Transparency (SD), Water Depth (D) and Ice Thickness (IT) were record directly on site. Total Nitrogen (TN), Total Phosphorus (TP), Dissolved Inorganic Phosphorus (DIP), Dissolved Total Phosphorus (DTP), Chlorophyll *a* (Chl.a), Suspended Solids (SS) of detection was carried out in the Inner Mongolia Water Resource Protection and Utilization Key Laboratory.

In January 2017, two irradiation monitors were installed at 1 m above the ice surface and 0.6 m below the ice surface at O10 in the

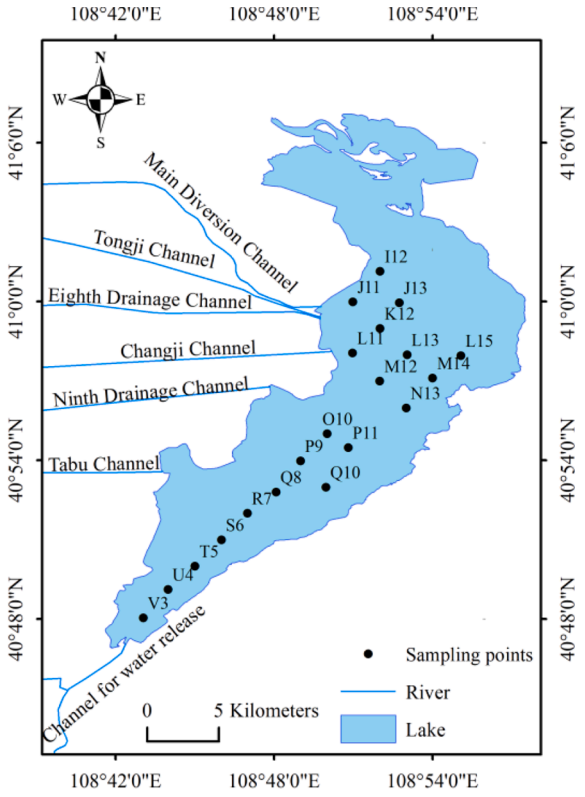

Fig. 1. Location of sampling points.

Table 1
Monitoring method or standard of indicators.

Indicators	Monitoring method or references
Water Temperature (WT), Salinity (S), pH, Electrical Conductance (EC), Total Dissolved Solids (TDS), Dissolved Oxygen (DO)	YSI Professional Plus
Transparency (SD)	Secchi Disk
Water Depth (D), Ice Thickness (IT)	Multi-Function Meter Ruler
Total Nitrogen (TN)	(Jiang, 2011)
Total Phosphorus (TP), Dissolved Inorganic Phosphorus (DIP), Dissolved Total Phosphorus (DTP)	(Jiang, 2011)
Chlorophyll *a* (Chl.a)	(Yu et al., 2021)
Suspended Solids (SS)	(Zhao et al., 2020)

center of the lake (the maximum ice thickness in January 2017 was 0.46 m, avoiding the freezing of the instrument) to collect photosynthetically active radiation (PAR) at the ice surface and ice-water interface during the ice period. At the same time, 10 temperature sensors were installed within 0.15–1.03 m above the water–sediment interface to fit the relationship between subglacial water temperature and water depth. The data of total radiation and light duration were obtained from the Australian-imported automatic weather station (MONITOR, AZWS-001) at the Main Diversion Channel of Wuliangsuhai Lake.

2.3. Calculations

The primary productivity calculation formula of the VGPM (Behrenfeld and Falkowski, 1997) is:

$$PP_{eu} = \begin{cases} 0.66125 P^{B}_{opt} \times \dfrac{E_0}{E_0 + 4.1} \times Z_{eu} \times C_{opt} \times D_{irr} \\ 0.66125 P^{B}_{opt} \times \dfrac{E_0}{E_0 + 4.1} \times Z_{eui} \times C_{opt} \times D_{irr} \end{cases} \quad (1)$$

where PP_{eu} (mg C•m^{-2}•d^{-1}) is the total primary productivity of the photic zone; P^{B}_{opt} (mg C•mg^{-1}Chl.a•h^{-1}) is the maximum carbon fixation rate, calculated by formula (2); E_0 is the PAR intensity (mol quanta•m^{-2}•d^{-1}) of the water surface (or ice-water interface), which is converted by total radiation. The monitored solar radiation wavelength is 320–950 nm, and the radiance at the wavelength of 400–700 nm was taken to calculate the PAR and applied to this study; Z_{eu} (m) is the depth of the photic zone in the ice-free period, which is calculated by formula (3). Z_{eui} (m) is the depth of the photic zone in the ice period, which is calculated by formula (4); C_{opt} is the concentration of chlorophyll-a (mg Chl.a•m^{-3}) at the depth of the maximum carbon fixation rate, which is replaced by the concentration of chlorophyll-a at 0.5 m below the water surface (or the ice-water interface); D_{irr} (h)is the duration of light from the automatic weather station.

$$P^{B}_{opt} = 1.2596 + 2.749 \times 10^{-1} WT + 6.17 \times 10^{-2} WT^2 - 2.05 \times 10^{-2} WT^3 + 2.46 \times 10^{-3} WT^4 - 1.348 \times 10^{-4} WT^5 + 3.4132 \times 10^{-6} WT^6 - 3.27 \times 10^{-8} WT^7 \quad (2)$$

In the formula (Behrenfeld and Falkowski, 1997), WT is the water temperature (℃) at the maximum carbon fixation rate of carbon in the photic zone. The water temperature uses the data at 0.5 m below the water surface in the ice-free period, and the fitting data of the water temperature and the distance from the water–sediment interface is used in the ice period, calculated after determining the depth of the photic zone in the ice period.

The simplified calculation formula of the photic zone depth in the ice-free period is as follows:

$$Z_{eu} = \frac{4.605 \times SD}{f} \quad (3)$$

The simplified calculation formula of the photic zone depth in the ice period is as follows:

$$Z_{eui} = -\frac{SD}{f} \ln \frac{14 e^{K_i(PAR)IT}}{(1 - R_s) E_d(0, PAR)} \quad (4)$$

In the formula, SD is transparency (m); f is the photosynthetically effective diffuse attenuation coefficient, f = 1.4 (Ma, 2016). K_i (PAR) is the ice extinction coefficient, K_i (PAR) = 4.66 m^{-1} (Tian, 2020); IT is ice thickness (m); R_s is the ice surface refractive index, taking 5 %; E_d (0, PAR) is the effective radiation of the ice surface.

In this study, spring refers to April, summer refers to July, autumn refers to October, winter refers to January of the following year, and all data are reported as the mean ± standard error (SE). Before statistical analysis, the single-sample Kolmogorov-Smirnov method and the Bartlett method were used to test the data for normality and variance homogeneity. The differences in primary productivity and environmental factors were tested in different spatiotemporal conditions by multiple comparisons using the analysis of variance (ANOVA) and LSD methods. RDA was used to analyze the relationship between PP_{eu} and environmental factors, and MLR was used to fit the functional relationship between PP_{eu} and environmental factors. Data standardization was performed using z-score standardization, new data = (original data-mean)/standard deviation. In RDA, a variable selection process was added to the constrained ranking to filter suitable explanatory variables. The variable selection method is forward selection, the Monte Carlo permutation tests were run to test the significance of each explanatory variable, and the explanatory variables were added to the ranking model one by one. SPSS Statistics 22 and Canoco 5 were used for the above analysis. Data mapping and visualization were conducted with ArcGIS 10.8 and Origin 2019b.

3. Results

3.1. Environmental factors

The results of variance analysis are summarized in Table 2. TN in winter was significantly higher than that in autumn, summer, and spring. The TN in autumn, summer, and spring was consistent with a class IV water quality (Surface Water Environmental Quality Standard GB3838-2020), whereas the water quality in winter decreased to class V. There was no significant difference in the TP of the four seasons, all of which were class IV water. The SS value in winter was significantly higher than that in summer and autumn, and SS in spring was in the middle. There were significant differences in WT in the four seasons, summer > spring > autumn > winter, and the lowest water temperature in winter could drop to 0.70 ± 0.10 °C. SD in autumn and spring were significantly higher than that in summer and winter. The DO values of the four seasons were significantly different, winter > autumn > spring > summer, and the DO values of the four seasons were all above the class II water standard. TDS in winter was significantly higher than that in spring, autumn, and summer. The pH values in autumn, spring, and summer were significantly higher than that in winter, and the water was weakly alkaline in all seasons. The D values in summer, spring, and autumn were significantly higher than in winter. The ice thickness formed by low temperatures in winter was 0.43 ± 0.01 m.

3.2. Vertical water temperature fitting under the ice

The data of 10 temperature sensors located within 0.15–0.95 m above the water–sediment interface at O10 are shown in Fig. 2a. The closer the distance to the water–sediment interface, the higher the WT. Therefore, the maximum value of WT appeared at the bottom of the photic zone in winter, and P^{B}_{opt} also appeared at the bottom of the photic zone. Fitting the arithmetic average of the 10-layer WT (January 1 to 31, 2017) with the distance from the water–sediment interface during the

Table 2
Seasonal variations of environmental factors (mean ± SE, Min – Max).

Environmental factors	Spring	Summer	Autumn	Winter
TN (mg•L^{-1})	1.42 ± 0.11^{b}	1.46 ± 0.05^{b}	1.68 ± 0.06^{b}	2.79 ± 0.35^{a}
	0.28–9.65	0.08–2.96	0.21–3.68	0.25–17.15
TP (mg•L^{-1})	0.09 ± 0.01^{a}	0.07 ± 0.01^{a}	0.06 ± 0.00^{a}	0.09 ± 0.01^{a}
	0.02–1.01	0.02–0.35	0.02–0.16	0.02–0.39
DIP (mg•L^{-1})	0.02 ± 0.00^{a}	0.03 ± 0.00^{a}	0.03 ± 0.00^{a}	0.02 ± 0.00^{b}
	0–0.24	0–0.11	0–0.09	0–0.23
DTP (mg•L^{-1})	0.04 ± 0.01^{a}	0.03 ± 0.00^{a}	0.03 ± 0.00^{a}	0.03 ± 0.00^{a}
	0–0.43	0–0.16	0.01–0.09	0–0.27
SS (mg•L^{-1})	20.21 ± 1.86^{ab}	14.91 ± 1.38^{b}	14.10 ± 1.47^{b}	29.08 ± 4.24^{a}
	0.00–84.00	1.00–78.00	0.00–95.00	0.30–229.00
WT (℃)	19.08 ± 0.31^{b}	25.31 ± 0.18^{a}	4.74 ± 0.18^{c}	0.70 ± 0.10^{d}
	12.30–25.20	22.50–30.10	2.00–12.20	−0.30–3.70
SD (m)	1.06 ± 0.05^{a}	0.91 ± 0.03^{b}	1.08 ± 0.04^{a}	0.80 ± 0.03^{b}
	0.25–2.50	0.16–1.69	0.10–1.93	0.37–1.76
Cond (mS•cm^{-1})	3.28 ± 0.10^{ab}	2.99 ± 0.12^{b}	2.34 ± 0.07^{c}	3.43 ± 0.14^{a}
	1.13–6.75	0.20–6.66	0.02–4.57	0.89–6.56
DO (mg•L^{-1})	8.47 ± 0.35^{b}	6.23 ± 0.28^{c}	10.26 ± 0.13^{a}	12.08 ± 0.61^{d}
	3.00–17.25	0.04–13.43	7.09–13.28	0.85–32.95
TDS (mg•L^{-1})	1.72 ± 0.05^{b}	1.54 ± 0.06^{b}	1.55 ± 0.06^{b}	2.35 ± 0.08^{a}
	0.60–3.36	0.58–3.26	0.02–3.35	0.43–4.11
S (psu)	1.71 ± 0.06^{b}	1.59 ± 0.07^{bc}	1.41 ± 0.04^{c}	2.12 ± 0.06^{a}
	0.06–3.68	0.06–3.68	0.01–2.77	0.36–3.35
pH	8.45 ± 0.04^{a}	8.42 ± 0.04^{a}	8.52 ± 0.03^{a}	8.12 ± 0.04^{b}
	7.34–9.60	7.50–9.51	7.18–9.17	6.77–8.95
D (m)	2.17 ± 0.05^{a}	2.24 ± 0.06^{a}	2.08 ± 0.06^{a}	1.83 ± 0.06^{b}
	1.37–3.98	1.06–5.40	1.07–3.70	0.40–3.28
IT (m)	/	/	/	0.43 ± 0.01
	/	/	/	0.22–0.60

Note: Different superscript letters in the same line indicate significant differences ($P < 0.05$, $n = 98$).

ice period, the results showed (Fig. 2b) that the relationship between the WT under the ice and the distance from the water–sediment interface is as follows: WT = 6.90 + 2.03x-11.89x^2 + 18.59x^3-25.13x^4 + 16.05x^5-3.23x^6(R^2 = 0.999). This formula was used to estimate WT and P^B_{opt} at the bottom of the photic zone during the ice period.

3.3. PP_{eu} parameters

The PAR, Z_{eu}, Chl.a, and D_{irr} of the 20 sampling points in Wuliangsuhai Lake are shown in Fig. 3. The PAR values of the four seasons were significantly different ($P < 0.05$, $F = 2150.32$) and exhibited the following descending order: summer (54.88 ± 0.52^{a} mol quanta•m^{-2}•d^{-1}) > spring (51.84 ± 0.40^{b} mol quanta•m^{-2}•d^{-1}) > autumn (19.52 ± 0.88^{c} mol quanta•m^{-2}•d^{-1}) > winter (2.40 ± 0.11^{d} mol quanta•m^{-2}•d^{-1}). There were also significant differences in Z_{eu} in the four seasons ($P < 0.05$, $F = 63.63$): summer (2.05 ± 0.07^{a} m) > spring (2.04 ± 0.06^{a} m) > autumn (1.78 ± 0.05^{b} m) > winter (1.11 ± 0.05^{c} m). The D_{irr} of the four seasons was also significantly different ($P < 0.05$, $F = 7179.88$): summer (14.58 ± 0.01^{a} h) > spring (14.07 ± 0.05^{b} h) > autumn (10.80 ± 0.01^{c} h) > winter (9.9 ± 0.00^{d} h). There were also significant differences in Chl.a in the four seasons ($P < 0.05$, $F = 5.34$): winter (14.10 ± 1.42^{a} mg•m^{-3}) > summer (14.03 ± 1.24^{a} mg•m^{-3}) > autumn (13.66 ± 1.47^{a} mg•m^{-3}) > spring (8.16 ± 0.75^{b} mg•m^{-3}). There were significant differences in P^B_{opt} in four seasons ($P < 0.05$, $F = 871.01$): spring (6.22 ± 0.05^{a} mg•m^{-3}) > summer (5.29 ± 0.07^{b} mg•m^{-3}) > autumn (4.02 ± 0.04^{c} mg•m^{-3}) > winter (3.09 ± 0.02^{d} mg•m^{-3}).

3.4. Spatiotemporal variation of PP_{eu}

On the time scale, the annual average of PP_{eu} exhibited the following order: 2014 (1133.92 ± 432.46 mg C•m^{-2}•d^{-1}) > 2017 (1000.51 ± 456.31 mg C•m^{-2}•d^{-1}) > 2016 (432.85 ± 154.33 mg C•m^{-2}•d^{-1}) > 2015 (428.36 ± 192.53 mg C•m^{-2}•d^{-1}) > 2018 (331.75 ± 132.75 mg C•m^{-2}•d^{-1}). The maximum value of PP_{eu} was observed in the summer of 2017, up to 2296.11 mg C•m^{-2}•d^{-1}. The minimum value appeared in the winter of 2018, only 71.49 mg C•m^{-2}•d^{-1}(Fig. 4a). There were significant differences in the mean PP_{eu} of spring, summer, autumn, and winter ($P < 0.05$, $F = 54.74$) (Fig. 4b): summer (1279.89 ± 111.04 mg C•m^{-2}•d^{-1}) > spring (782.42 ± 59.34 mg C•m^{-2}•d^{-1}) > autumn (465.03 ± 49.30 mg C•m^{-2}•d^{-1}) > winter (96.34 ± 10.36 mg C•m^{-2}•d^{-1}).

On the spatial scale, the whole lake was divided into three parts: the north (I12, J11, J13, K12, *L*11, L13, L15), the central (M12, M14, N13, O10, P9, P11), and the south (Q8, Q10, R7, S6, T5, U4, V3) regions, as shown in Table. 3. There were significant differences in the PP_{eu} of the three parts in spring ($P < 0.05$, $F = 5.18$): north > central > south. There were no significant differences in the PP_{eu} of the three regions in summer ($P = 0.13$, $F = 2.36$): north > central > south. There were no significant differences in PP_{eu} in the three regions in autumn ($P = 0.30$, $F = 1.31$): south > north > central. There were no significant differences in the PP_{eu} of the three regions in winter ($P = 0.76$, $F = 0.28$): central > north > south.

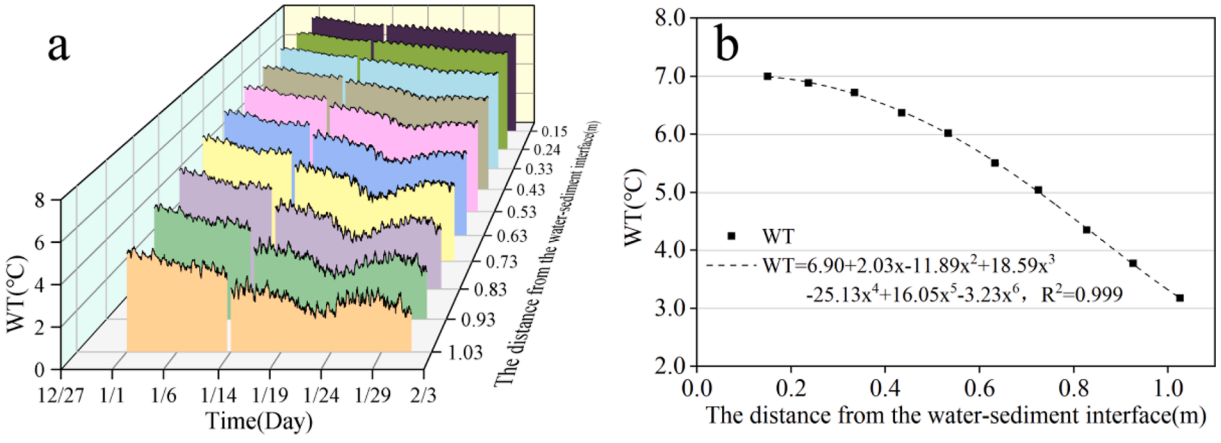

Fig. 2. The fitting of WT and distance from the water–sediment interface.

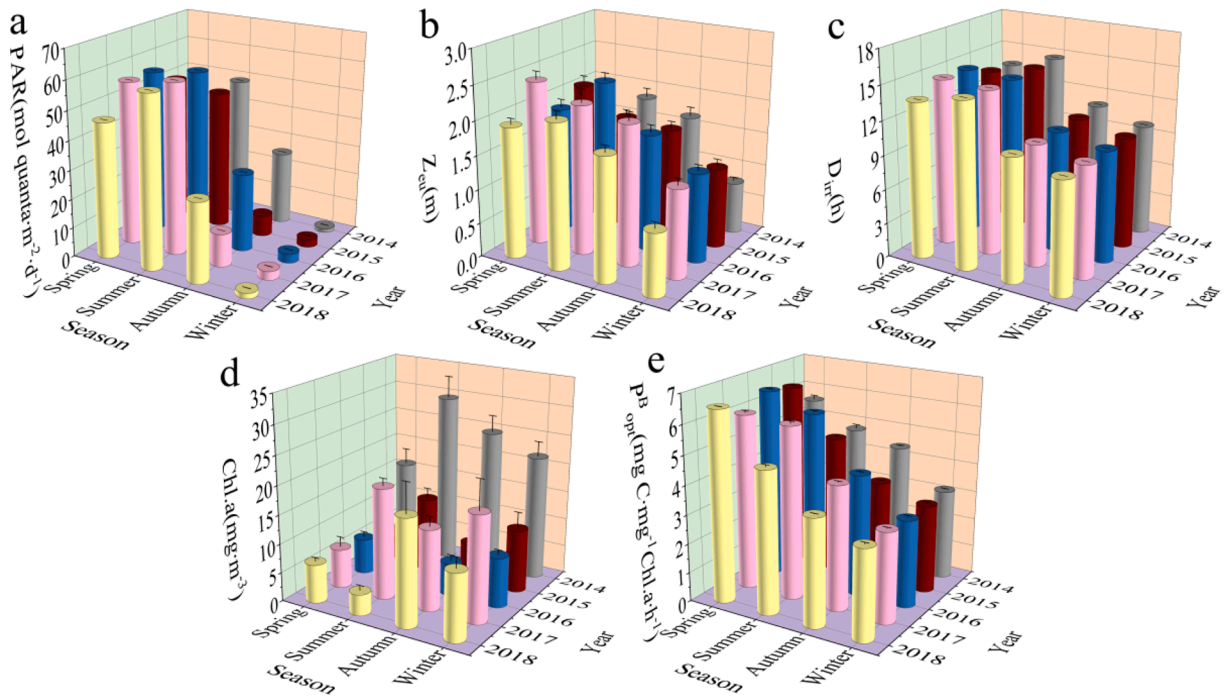

Fig. 3. Seasonal variations of PP_{eu} parameters.

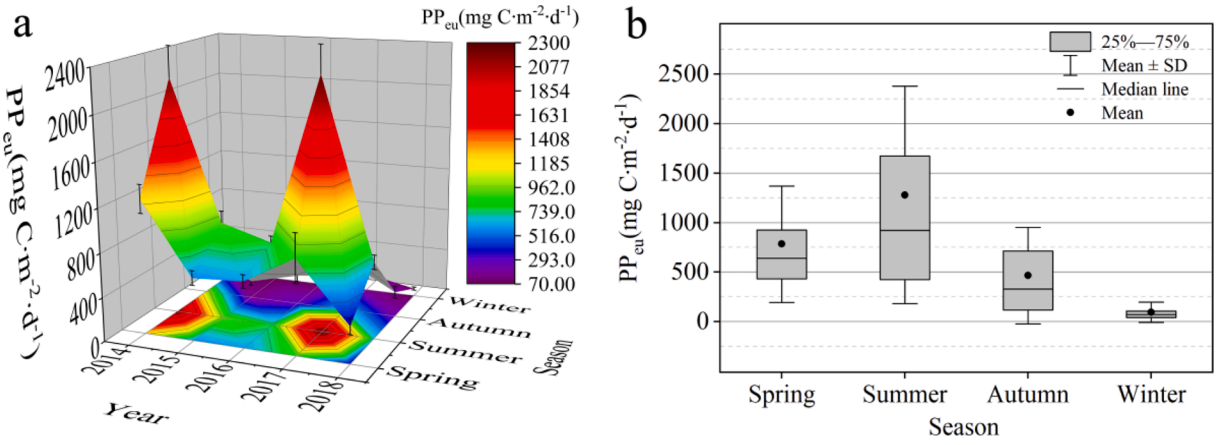

Fig. 4. The time variation of PP_{eu}.

Table 3
The spatial variations of PP_{eu} (mg C•m^{-2}•d^{-1}).

	North	Central	South
Spring	1034.91 ± 161.40^{a}	735.06 ± 34.43^{ab}	555.97 ± 71.37^{b}
Summer	1454.40 ± 183.11^{a}	1338.65 ± 163.24^{a}	1031.33 ± 67.62^{a}
Autumn	457.41 ± 41.27^{a}	375.19 ± 33.09^{a}	545.56 ± 109.91^{a}
Winter	96.75 ± 15.17^{a}	104.73 ± 22.69^{a}	86.82 ± 13.14^{a}

4. Discussion

To explore the main environmental factors affecting PP_{eu}, the data of PP_{eu} and environmental factors were standardized, with PP_{eu} as the dependent variable and environmental factors as the independent variables, after which RDA and MLR analysis were conducted. But in the final visualization, all explanatory variables (fit and unfit) were checked as controls. In MLR, environmental factors that are significantly correlated with PP_{eu} ($p < 0.05$) are preferentially selected as explanatory variables, and the explanatory variables are required to be independent of each other and there is no multicollinearity.

The RDA results are shown in Fig. 5. The eigenvalues of axis 1 and 2 in spring are 0.54 and 0.03, respectively. The selected environmental factors explain 57 % of the variation information of Chl.a. PP_{eu} was positively correlated with TN, TP, and DO. The eigenvalues of axis 1 and 2 in summer were 0.30 and 0.05, respectively. The selected environmental factors explain 35 % of the variation information of Chl.a, PP_{eu} was positively correlated with DIP, DO, S, and EC, and negatively correlated with WT. The eigenvalues of axis 1 and 2 in autumn were 0.24 and 0.03, respectively. The selected environmental factors explained 27 % of the variation information of Chl.a. PP_{eu} was positively correlated with pH, EC, WT, and TP. The eigenvalues of axis 1 and 2 in winter were 0.33 and 0.02, respectively. The selected environmental factors explained 35 % of the variation information of Chl.a. PP_{eu} was positively correlated with WT and negatively correlated with IT. Z_{eu} in the whole year had a good positive correlation with D and SD, and a negative correlation with SS, whereas Chl.a had a good positive correlation with TP and DO throughout the entire year.

The results of MLR analysis are shown in Table 4. The D-W index is

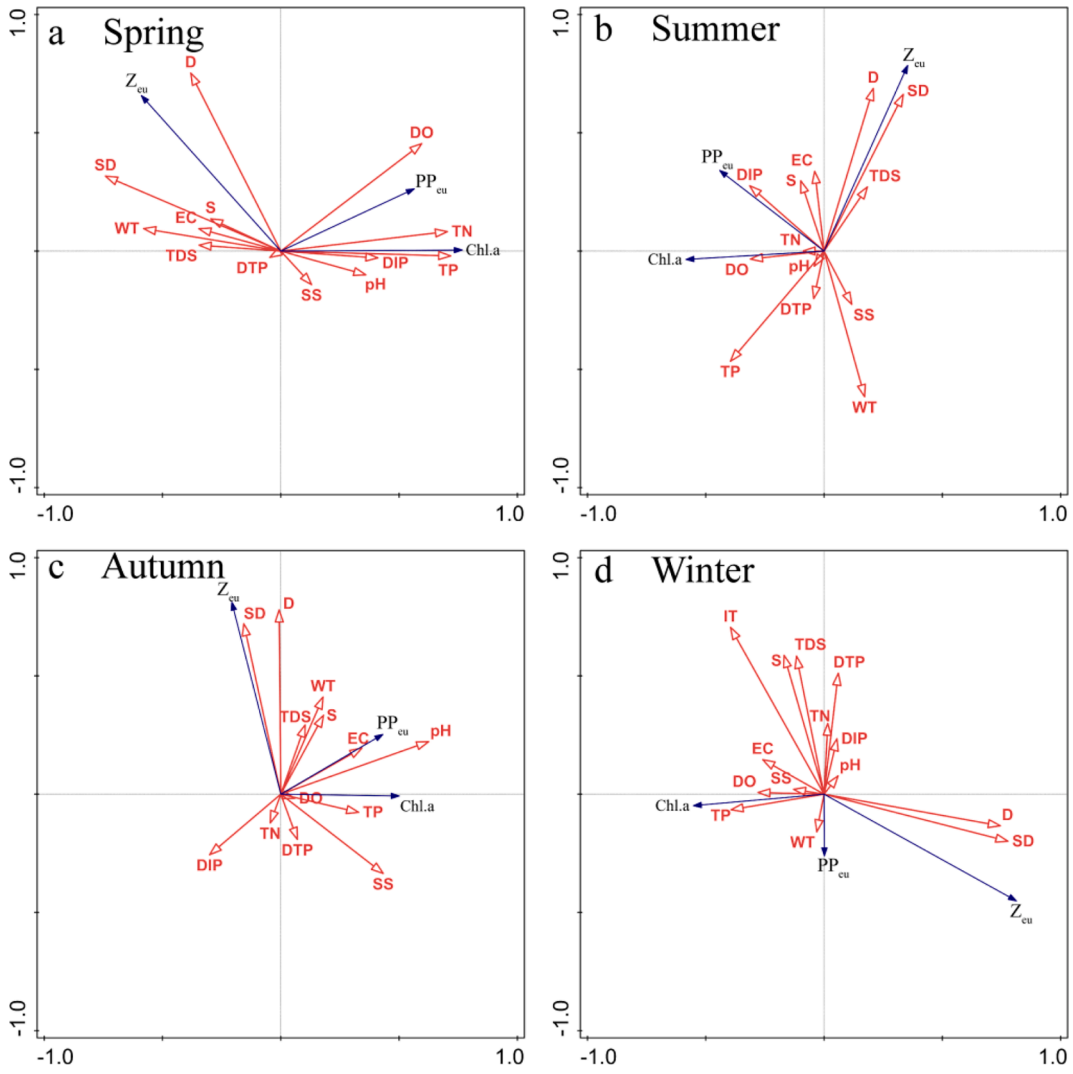

Fig. 5. Correlation analysis between PP_{eu} and environmental factors.

close to 2, and the VIF is<5. The sample independence test and multicollinearity test of environmental factors were all passed. Finally, the variation of PP_{eu} in spring can be revealed by Chl.a, TP, and Z_{eu} (R^2 = 0.82). The variation of PP_{eu} in summer can be revealed by Chl.a, Z_{eu} and WT (R^2 = 0.89). The variation of PP_{eu} in autumn can be revealed by Chl. a, Z_{eu}, and SS (R^2 = 0.69). The variation of PP_{eu} in winter can be revealed by Chl.a and Z_{eu} (R^2 = 0.88). Although the environmental factors driving PP_{eu} in the four seasons are different, it is clear that Chl.a and Z_{eu} are the main environmental factors affecting PP_{eu} throughout the year, and they determine the upper limit of PP_{eu} to different degrees. First, chlorophyll *a*, as the most important player in fixing inorganic carbon to organic carbon in phytoplankton, undoubtedly contributes the most to primary productivity. On the other hand, the space required for normal growth and reproduction of phytoplankton depends on Z_{eu}, especially in eutrophic shallow lakes like Wuliangsuhai Lake. When chemical factors (e.g., nutrients) are no longer the main environmental factors limiting the growth and reproduction of phytoplankton, the limiting factors often shift to physical factors (e.g., Z_{eu}). The higher the lake level, the greater the growth potential of Z_{eu} and the more room for phytoplankton activity, which tend to be higher in phytoplankton biomass and PP_{eu}. Therefore, the PP_{eu} of deep lakes is usually higher than that of shallow lakes. It can also be seen in the constructed multiple linear regression formula that the coefficient of Chl.a is the highest in spring, indicating that PP_{eu} in spring responds more strongly to the change of Chl.a. The coefficient of Z_{eu} is highest in winter, indicating that PP_{eu} is more sensitive to changes in Z_{eu} when ice sheets are present, which just confirms the negative effects of ice sheets on Z_{eu}.

Table 4
The multiple linear regression of the Zscore (PP_{eu}) and Zscore (environmental factors).

Season	Multiple linear regression formula	R^2	D-W index	VIF	F
Spring	$Zscore(PP_{eu}) = 1.21Zscore(Chl.a)-0.42Zscore(TP) + 0.24Zscore(Zeu)-4.8587E-16$	0.82	1.58	1.19–2.18	152.11
Summer	$Zscore(PP_{eu}) = 0.93Zscore(Chl.a) + 0.43Zscore(Z_{eu})-0.13Zscore(WT)-2.5199E-16$	0.89	1.20	1.11–1.26	252.66
Autumn	$Zscore(PP_{eu}) = 0.58Zscore(Chl.a) + 0.46Zscore(Z_{eu}) + 0.26Zscore(SS) + 4.105E-16$	0.69	1.27	1.03–1.18	39.27
Winter	$Zscore(PP_{eu}) = 0.91Zscore(Chl.a) + 0.47Zscore(Z_{eu}) + 8.88E-16$	0.88	1.48	1.115	158.25

Note: Zscore is standardized data; D-W index is Durbin-Watson index; VIF is variance inflation factor.

4.1. Driving factors of PP_{eu} temporal heterogeneity

In terms of temporal heterogeneity, WT is an important environmental factor affecting PP_{eu} (Kang et al., 2019; Morin et al., 1999). The photosynthesis of phytoplankton is a series of complex chemical reactions with the participation of a variety of enzymes (Teeling et al., 2012; Hopkinson et al., 2011), and the activity of enzymes is affected by temperature influences. The phytoplankton community in Wuliangsuhai Lake was dominated by green algae and diatoms. The optimal WT for the photosynthesis of most green algae is approximately 20 °C (Giannelli et al, 2015), whereas the optimal WT for diatom growth is between 10 and 25 °C (Cohn et al., 2003). Therefore, during autumn and winter (i.e., the low-temperature period), the enzyme activity increased with the increase of WT, and the metabolism, growth, reproduction, and nutrient absorption rate of phytoplankton were accelerated. Thus, PP_{eu} was positively correlated with WT in these two seasons. It should be noted that WT above a critical value will inhibit the photosynthetic rate of phytoplankton (Gonzalez-Olalla et al., 2022; Bouchard and Yamasaki, 2008). Additionally, the optimal growth temperature of the algae will also decrease with increased radiation intensity (Thorel et al., 2014) in the spring and summer (i.e., the high-temperature period). In turn, this continuous increase in water temperature begins to inhibit the photosynthetic rate of phytoplankton, and therefore WT is negatively correlated with PP_{eu}. Moreover, the vertical variation of WT exhibits opposite trends in the ice period and ice-free period. Particularly, the WT of the ice-water interface in the ice period is approximately 0 °C, the WT maximum appears at the water–sediment interface, and the WT at the bottom of Z_{eu} is only 0.70. ± 0.10 °C. This low temperature significantly inhibits the photosynthetic rate of phytoplankton and decreases PP_{eu}.

Nutrients play an indispensable role for phytoplankton during photosynthesis (Burson et al., 2018). In spring, the temperature rises and the ice sheet begins to melt, and the nitrogen and phosphorus pollutants that had attached to the ice surface through atmospheric deposition during the ice period enter the water. At the same time, the melting of the ice sheet increases external interference, and the sediment becomes the source of nutrients in the water (Lutgen et al., 2020; Ahiablame et al., 2010). Abiotic factors such as wind speed, air temperature, and hydrodynamics make the nutrients in the sediment migrate to water (Khirul et al., 2021; Li et al., 2021). Summer is a period of concentrated precipitation in Wuliangsuhai Lake throughout the year. The surface runoff formed by the rainfall transports the nutrients in the land area and enters the water. Additionally, the continuous high-temperature weather sharply increases the water surface evaporation, the water continues to concentrate, and the nutrient concentration increases. In autumn, Wuliangsuhai Lake receives the retreating water from Hetao Irrigation District, and the retreating water contains a large amount of ammonia nitrogen, phosphorus, pesticides, and chemical fertilizer residues (Shi et al., 2020), resulting in higher TN content in autumn water than in summer. In winter, the severe cold leads to the formation of an ice sheet of 0.43 ± 0.01 m in Wuliangsuhai Lake. The salt discharge effect of the ice sheet caused the nutrients in the ice to be precipitated. The concentration of nutrients at the ice-water interface was higher than that of the lower water, and the resulting concentration difference forced the nutrients to diffuse downwards (Zhang et al., 2013). Finally, TN and TP reached their highest year-round values in winter. The annual TP content in Wuliangsuhai Lake was between 0.06 and 0.09 mg•L^{-1}, and the TN content was between 1.42 and 2.79 mg•L^{-1}. Under the influence of high nutrient concentrations, phytoplankton did not reach the highest carrying capacity of nutrients in most periods, and PP_{eu} was affected by factors other than nutrients, such as light, temperature, wind speed, and other physical conditions. Therefore, the RDA and MLR results indicated that TP and TN could not significantly affect PP_{eu} in other seasons except spring.

Studies have shown that there is usually a positive correlation between DO concentration and algae density in water (Hilaluddin et al., 2020), and the annual DO also showed a good correlation with Chl.a in this study. Since the WT in Wuliangsuhai Lake rose to the highest value in summer, the DO in summer was significantly lower than that in winter, autumn, and spring, but still higher than the surface water class II water standard. The seasonal variation of D_{irr}, PAR, and PP_{eu} was consistent, exhibiting the following order: summer > spring > autumn > winter.

Z_{eu} takes the actual water depth as the upper limit. The annual Z_{eu} has a good positive correlation with D and SD, and a negative correlation with SS. In waters with weak hydrodynamic conditions, suspended particles are more likely to migrate from the water to the sediment (Ma et al., 2021), and SD increases. This makes it easier for Z_{eu} and PAR to extend to the lower part of the water, which benefits the growth of phytoplankton. However, Z_{eu} is negatively correlated with IT in winter. The existence of an ice sheet greatly weakens the O_2-CO_2 exchange between the water and the atmosphere, and also greatly weakens Z_{eu} and PAR under the ice. Z_{eu} in winter was only 1.11 ± 0.05 m and the PAR value was only 2.40 ± 0.11 mol quanta•m^{-2}•d^{-1}, which were significantly lower than those in summer, spring, and autumn. Therefore, the overall level of PP_{eu} in winter was lower. Although high nutrient concentrations provide favorable conditions for phytoplankton photosynthesis in winter, the highest DO concentration (12.08 ± 0.61 mg•L^{-1}) also appeared in winter, which compensated for phytoplankton photosynthesis to a certain extent. However, due to the limitation of environmental factors such as WT, IT, and Z_{eu}, the PP_{eu} in winter was significantly lower than that in other seasons.

4.2. Driving factors of PP_{eu} spatial heterogeneity

In terms of spatial heterogeneity, significant differences in the spatial distribution of PP_{eu} were found only in spring (north > central > south). The distribution of reeds, the geographic location of drainage, and hydrodynamic conditions are the main environmental factors affecting PP_{eu}. Reeds in Wuliangsuhai Lake are mainly distributed in the Xiaohaizi area in the north where no sampling points are laid, the main diversion channel area, and the central area. The ice sheet melted in spring, and the water in Wuliangsuhai Lake and the water outside the lake began to gradually exchange. The Bayan Nur section of the Yellow River also provides ecological hydration to Wuliangsuhai Lake every spring. >90 % of the water is drained from the main diversion channel into Wuliangsuhai Lake. It flows through the central region and then flows out from the southern drainage channel. Because the reeds of the main diversion channel and the middle region are denser than in other waters, the water flow rate is slow, and N and P nutrients are enriched in this area (Quan et al., 2019). PP_{eu} has a good correlation with TN and TP in spring. Additionally, the waters with weaker hydrodynamic conditions had higher SD, Z_{eu}, and PAR. Therefore, these waters were more suitable for the growth and reproduction of phytoplankton (Yu et al., 2015), with the PP_{eu} in the north and the central regions being significantly higher than that in the south. The nutrient concentration in summer and autumn was higher, and nutrients were therefore no longer the limiting factor of PP_{eu}. At this time, there was no significant difference in the spatial distribution of environmental factors, and therefore there is no significant difference in the spatial distribution of PP_{eu}. Under the influence of the ice sheet and the low temperatures in winter, the PP_{eu} of the whole lake was lower and there was no significant difference. However, PP_{eu} could still reach 8 % in summer.

5. Conclusions

The annual average PP_{eu} values of Wuliangsuhai Lake in spring, summer, autumn, and winter were 782.42 ± 59.34 mg C•m^{-2}•d^{-1}, 1279.89 ± 111.04 mg C•m^{-2}•d^{-1}, 465.03 ± 49.30 mg C•m^{-2}•d^{-1}, and 96.34 ± 10.36 mg C•m^{-2}•d^{-1}, respectively. The PP_{eu} of Wuliangsuhai Lake had strong temporal heterogeneity, and the PP_{eu} of the four seasons was significantly different, exhibiting the following order: summer > spring > autumn > winter. Spatial heterogeneity was weak, and only the

PP_{eu} of spring had significant differences: north > central > south. There were no significant spatial differences in PP_{eu} in summer, autumn, and winter. The environmental factors affecting PP_{eu} in Wuliangsuhai Lake were different in the four seasons. In spring, PP_{eu} was mainly affected by TN, TP, and DO, and the increase of these three factors promoted PP_{eu}. In summer, PP_{eu} was mainly affected by DIP, DO, S, EC, and WT, and the increase of the first four could promote the increase of PP_{eu}. However, under the condition of high radiation, the optimal growth temperature of phytoplankton decreased, and the increase of WT would inhibit the growth of phytoplankton, which led to the decrease of PP_{eu}. In autumn, PP_{eu} was mainly affected by pH, EC, SS, and WT, and the increase of these four parameters promoted PP_{eu}. In winter, PP_{eu} was mainly affected by WT and IT. The increase of WT can promote PP_{eu}, and the increase of IT seriously weakened PAR, Z_{eu}, and the O_2-CO_2 exchange capacity of lake water and atmosphere, thus inhibiting PP_{eu}. Although the growth and reproduction of phytoplankton in winter faces great challenges, the PP_{eu} under the ice sheet can reach 8 % of that in summer.

CRediT authorship contribution statement

Haifeng Yu: Investigation, Software, Visualization, Writing – original draft. **Xiaohong Shi:** Conceptualization, Funding acquisition. **Shengnan Zhao:** Conceptualization, Resources. **Biao Sun:** Formal analysis. **Yu Liu:** Validation. **Lauri Arvola:** Validation. **Guohua Li:** Investigation, Project administration. **Yanjun Wang:** Investigation, Visualization. **Xueru Pan:** Investigation, Visualization. **Rong Wu:** Data curation, Visualization. **Zhiqiang Tian:** Investigation, Visualization.

Declaration of Competing Interest

The authors declare that they have no known competing financial interests or personal relationships that could have appeared to influence the work reported in this paper.

Data availability

The authors do not have permission to share data.

Acknowledgements

This work was supported by the National Key Research and Development Program of China (2017YFE0114800; 2019YFC0409200); The National Natural Science Foundation of China (52260028; 52060022; 51869020; 51909123); The Inner Mongolia Autonomous Region Science and Technology Plan (2021GG0089). The authors would like to thank all the reviewers who participated in the review, as well as MJEditor (www.mjeditor.com) for providing English editing services during the preparation of this manuscript.

References

Ahiablame, L., Chaubey, I., Smith, D., 2010. Nutrient content at the sediment-water interface of tile-fed agricultural drainage ditches. Water 2 (3), 411–428.
Behrenfeld, M.J., Falkowski, P.G., 1997. Photosynthetic rates derived from satellite-based chlorophyll concentration. Limnol. Oceanogr. 42 (1), 1–20.
Behrenfeld, M.J., O'Malley, R.T., Siegel, D.A., McClain, C.R., Sarmiento, J.L., Feldman, G.C., Milligan, A.J., Falkowski, P.G., Letelier, R.M., Boss, E.S., 2006. Climate-driven trends in contemporary ocean productivity. Nature 444 (7120), 752–755.
Bondarenko, N.A., Timoshkin, O.A., Röpstorf, P., Melnik, N.G., 2006. The under-ice and bottom periods in the life cycle of Aulacoseira baicalensis (K. Meyer) Simonsen, a principal Lake Baikal alga. Hydrobiologia 568 (S1), 107–109.
Bouchard, J.N., Yamasaki, H., 2008. Heat stress stimulates nitric oxide production in Symbiodinium microadriaticum: a possible linkage between nitric oxide and the coral bleaching phenomenon. Plant Cell Physiol. 49 (4), 641–652.
Brown, R.D., Hughes, M.G., Robinson, D.A., 1995. Characterizing the long-term variability of snow-cover extent over the interior of North America. Ann. Glaciol. 21, 45–50.
Burson, A., Stomp, M., Greenwell, E., Grosse, J., Huisman, J., 2018. Competition for nutrients and light: testing advances in resource competition with a natural phytoplankton community. Ecology 99 (5), 1108–1118.
Canfield, D.E., Bachmann, R.W., Hoyer, M.V., 1983. Freeze-out of salts in hard-water lakes1. Limnol. Oceanogr. 28 (5), 970–977.
Cohn, S.A., Farrell, J.F., Munro, J.D., Ragland, R.L., Weitzell, R.E., Wibisono, B.L., 2003. The effect of temperature and mixed species composition on diatom motility and adhesion. Diatom Res. 18 (2), 225–243.
Cox, T.J.S., Maris, T., Soetaert, K., Kromkamp, J.C., Meire, P., Meysman, F., 2015. Estimating primary production from oxygen time series: a novel approach in the frequency domain. Limnol. Oceanogr.-Methods 13 (10), 529–552.
Delu, P., Wenjiang, G., Yan, B., Haiqing, H., 2005. Ocean primary productivity estimation of China Sea by remote sensing. Prog. Nat. Sci. 15 (7), 627–632.
Everett, J.D., Doblin, M.A., 2015. Characterising primary productivity measurements across a dynamic western boundary current region. Deep-Sea Res. Part I-Oceanogr. Res. Papers 100, 105–116.
Giannelli, L., Yamada, H., Katsuda, T., Yamaji, H., 2015. Effects of temperature on the astaxanthin productivity and light harvesting characteristics of the green alga *Haematococcus pluvialis*. J. Biosci. Bioeng. 119 (3), 345–350.
Gonzalez-Olalla, J.M., Medina-Sanchez, J.M., Carrillo, P., 2022. Fluctuation at high temperature combined with nutrients alters the thermal dependence of phytoplankton. Microb. Ecol. 83 (3), 555–567.
Grenfell, T.C., Perovich, D.K., 1984. Spectral albedos of sea ice and incident solar irradiance in the southern Beaufort Sea. J. Geophys. Res. 89, 3573–3580.
Guo, X.J., Xi, B.D., Yu, H.B., Ma, W.C., He, X.S., 2011. The structure and origin of dissolved organic matter studied by UV-vis spectroscopy and fluorescence spectroscopy in lake in arid and semi-arid region. Water Sci. Technol. 63 (5), 1010–1017.
Hampton, S.E., Galloway, A.W.E., Powers, S.M., Ozersky, T., Woo, K.H., Batt, R.D., Labou, S.G., O'Reilly, C.M., Sharma, S., Lottig, N.R., Stanley, E.H., North, R.L., Stockwell, J.D., Adrian, R., Weyhenmeyer, G.A., Arvola, L., Baulch, H.M., Bertani, I., Bowman, L.L., Carey, C.C., Catalan, J., Colom-Montero, W., Domine, L.M., Felip, M., Granados, I., Gries, C., Grossart, H.-P., Haberman, J., Haldna, M., Hayden, B., Higgins, S.N., Jolley, J.C., Kahilainen, K.K., Kaup, E., Kehoe, M.J., MacIntyre, S., Mackay, A.W., Mariash, H.L., McKay, R.M., Nixdorf, B., Nõges, P., Nõges, T., Palmer, M., Pierson, D.C., Post, D.M., Pruett, M.J., Rautio, M., Read, J.S., Roberts, S. L., Rücker, J., Sadro, S., Silow, E.A., Smith, D.E., Sterner, R.W., Swann, G.E.A., Timofeyev, M.A., Toro, M., Twiss, M.R., Vogt, R.J., Watson, S.B., Whiteford, E.J., Xenopoulos, M.A., Grover, J., 2017. Ecology under lake ice. Ecol. Lett. 20 (1), 98–111.
Hancke, K., Lund-Hansen, L.C., Lamare, M.L., Højlund Pedersen, S., King, M.D., Andersen, P., Sorrell, B.K., 2018. Extreme low light requirement for algae growth underneath sea ice: a case study from station Nord, NE Greenland: MINIMUM LIGHT REQUIREMENT FOR ICE ALGAE. J. Geophys. Res. 123 (2), 985–1000.
Hawes, I., Schwarz, A.M.J., 2001. ABSORPTION AND UTILIZATION OF IRRADIANCE BY CYANOBACTERIAL MATS IN TWO ICE-COVERED ANTARCTIC LAKES WITH CONTRASTING LIGHT CLIMATES. J. Phycol. 37 (1).
Hilaluddin, F., Yusoff, F.M., Natrah, F.M.I., Lim, P.T., 2020. Disturbance of mangrove forests causes alterations in estuarine phytoplankton community structure in Malaysian Matang mangrove forests. Mar. Environ. Res. 158, 104935.
Hopkinson, B.M., Dupont, C.L., Allen, A.E., Morel, F.M., 2011. Efficiency of the CO_2-concentrating mechanism of diatoms. Proc. Natl. Acad. Sci. USA 108 (10), 3830–3837.
Huan, Y., Sun, D.Y., Wang, S.Q., Zhang, H.L., Qiu, Z.F., Bilal, M., He, Y.J., 2021. Remote sensing estimation of phytoplankton absorption associated with size classes in coastal waters. Ecol. Ind. 121, 107198.
Jia, J., Gao, Y., Lu, Y., Shi, K., Li, Z., Wang, S., 2020. Trace metal effects on gross primary productivity and its associative environmental risk assessment in a subtropical lake, China. Environ. Pollut. 259, 113848.
Jiang, H.Q., 2011. Experimental Study on the Spatial Distribution of Nutrient Salts in the Ice of Lake Wuliangsuhai and Their Release Processes during Melting. Inner Mongolia Agricultural University, Hohhot. In Chinese.
Kang, Y., Kang, H.Y., Kim, D., Lee, Y.J., Kim, T.I., Kang, C.K., 2019. Temperature-dependent bifurcated seasonal shift of phytoplankton community composition in the coastal water off Southwestern Korea. Ocean Sci. J. 54 (3), 467–486.
Khirul, M.A., Kim, B.-G., Cho, D., Kwon, S.-H., 2021. Distribution of vital, environmental components and nutrients migration over sedimentary water layers. J. Environ. Sci.-China 30 (3), 195–206.
Lakshmi, E., Pratap, D., Nagamani, P.V., Rao, K.H., Latha, T.P. and Choudhury, S.B. (2014) TIME SERIES ANALYSIS OF PRIMARY PRODUCTIVITY ALONG THE EAST COAST OF INDIA USING OCEANSAT-2 OCEAN COLOUR MONITOR (OCM), pp. 1049-1053, Copernicus Gesellschaft Mbh, Hyderabad, INDIA.
Lan, K.W., Lian, L.J., Li, C.H., Hsiao, P.Y., Cheng, S.Y., 2020. Validation of a primary production algorithm of vertically generalized production model derived from multi-satellite data around the waters of Taiwan. Remote Sens. 12 (10), 1627.
Li, X.J., Zhao, Y.P., Han, R.M., Wang, G.X., 2021. Fractionation and determinants of sediment nitrogen and phosphorus in the algae-dominated Moon bay of lake Taihu (China). J. Coastal Res. 37 (3), 506–517.
Lutgen, A., Jiang, G., Sienkiewicz, N., Mattern, K., Kan, J.J., Inamdar, S., 2020. Nutrients and heavy metals in legacy sediments: concentrations, comparisons with upland soils, and implications for water quality. J. Am. Water Resour. Assoc. 56 (4), 669–691.
Ma, Z.H., Wang, L., Li, X.Y., Qu, X.N., Yin, J., Zhao, X.I., Liu, Y.Q., 2021. The oasis regional small and medium lake water transparency monitoring research and impact factor analysis based on field data combined with high resolution GF-1 satellite data. J. Freshwater Ecol. 36 (1), 77–96.

Ma, J.X. (2016) Inversion of Kd(PAR) and euphotic zone depth of typical water bodys in Northeast China with remote imagery, Graduate University of Chinese Academy of Sciences (Northeast Institute of Geography and Agroecology), Changchun. (In Chinese).

Morin, A., Lamoureux, W., Busnarda, J., 1999. Empirical models predicting primary productivity from chlorophyll a and water temperature for stream periphyton and lake and ocean phytoplankton. J. North Am. Benthol. Soc. 18 (3), 299–307.

Perovich, D.K., 2003. Complex yet translucent: the optical properties of sea ice. Phys. B-Condens. Matter 338 (1–4), 107–114.

Popovskaya, G.I., 2000. Ecological monitoring of phytoplankton in Lake Baikal. Aquat. Ecosyst. Health Manage. 3, 215–225.

Pratt, D.M., Berkson, HAROLD, 1959. Two sources of error in the oxygen light and dark bottle method. Limnol. Oceanogr. 4 (3), 328–334.

Quan, D., Shi, X.H., Zhao, S.N., Zhang, S., Liu, J.J., 2019. Eutrophication of Lake Ulansuhai in 2006–2017 and its main impact factors. J. Lake Sci. 31 (5), 1259–1267.

Schagerl, M., Oduor, S.O., 2003. On the limnology of Lake Baringo (Kenya): II. Pelagic primary production and algal composition of Lake Baringo, Kenya. Hydrobiologia 506 (1–3), 297–303.

Sharma, S., Blagrave, K., Filazzola, A., Imrit, M.A., Franssen, H.J.H., 2021. Forecasting the permanent loss of lake ice in the northern hemisphere within the 21st century. Geophys. Res. Lett. 48 (1) e2020GL091108.

Shi, R., Zhao, J., Shi, W., Song, S., Wang, C., 2020. Comprehensive assessment of water quality and pollution source apportionment in Wuliangsuhai Lake, Inner Mongolia, China. Int J Environ Res Public Health 17 (14), 5054.

Song, S., Li, C.Y., Shi, X.H., Zhao, S.N., Tian, W.D., Li, Z.J., Bai, Y.L., Cao, X.W., Wang, Q. K., Huotari, J., Tulonen, T., Uusheimo, S., Lepparanta, M., Loehr, J., Arvola, L., 2019. Under-ice metabolism in a shallow lake in a cold and arid climate. Freshw. Biol. 64 (10), 1710–1720.

Teeling, H., Fuchs, B.M., Becher, D., Klockow, C., Gardebrecht, A., Bennke, C.M., Kassabgy, M., Huang, S., Mann, A.J., Waldmann, J., Weber, M., Klindworth, A., Otto, A., Lange, J., Bernhardt, J., Reinsch, C., Hecker, M., Peplies, J., Bockelmann, F. D., Callies, U., Gerdts, G., Wichels, A., Wiltshire, K.H., Glockner, F.O., Schweder, T., Amann, R., 2012. Substrate-controlled succession of marine bacterioplankton populations induced by a phytoplankton bloom. Science 336 (6081), 608–611.

Terzhevik, A., Golosov, S., Palshin, N., Mitrokhov, A., Zdorovennov, R., Zdorovennova, G., Kirillin, G., Shipunova, E., Zverev, I., 2009. Some features of the thermal and dissolved oxygen structure in boreal, shallow ice-covered Lake Vendyurskoe, Russia. Aquat. Ecol. 43 (3), 617–627.

Thorel, M., Fauchot, J., Morelle, J., Raimbault, V., Le Roy, B., Miossec, C., Kientz-Bouchart, V., Claquin, P., 2014. Interactive effects of irradiance and temperature on growth and domoic acid production of the toxic diatom Pseudo-nitzschia australis (Bacillariophyceae). Harmful Algae 39, 232–241.

Tian, W.D., 2020. Simulation and Analysis on the Euphotic Zone and Primary Productivity of phytoplankton in Wuliangsuhai. Inner Mongolia Agricultural University, Hohhot. In Chinese.

Westernhagen, N., Hamilton, D.P., Pilditch, C.A., 2010. Temporal and spatial variations in phytoplankton productivity in surface waters of a warm-temperate, monomictic lake in New Zealand. Hydrobiologia 652 (1), 57–70.

Yu, Q., Chen, Y.C., Liu, Z.W., van de Giesen, N., Zhu, D.J., 2015. The influence of a eutrophic lake to the river downstream: spatiotemporal algal composition changes and the driving factors. Water 7 (5), 2184–2201.

Yu, H.F., Shi, X.H., Sun, B., Zhao, S.N., Liu, Y., Zhao, M.L., 2021. Analysis of water quality and eutrophication changes in Hulun Lake from 2011 to 2020. Arid Zone Res. 38 (06), 1534–1545.

Zhang, Y., Li, C.Y., Shen, H.T., Shi, X.H., Qiao, L.M., 2013. Total nitrogen migration in Wuliangsuhai Lake during ice growth process. Adv. Water Sci. 24 (05), 728–735.

Zhao, L., Yu, J.W., Xing, J.Y., Wang, S.H., Cai, Q., Zheng, S.F., Jiang, X., 2020. Spatial and temporal distribution characteristics and environmental effects of suspended solids in Nanhu Lake. J. Environ. Eng. Technol. 10 (6), 905–911.